Original Research Paper   **Open Access**

A Project Design for Air Pollution Studies Over Bobodioulasso-Burkina Faso

Emetere M.E. *(****), Sanni S.E. and Okoro E.E.****

*Department of Physics, Covenant University, P.M.B 1023, Ota, Nigeria
**Department of Chemical Engineering, Covenant University, Canaan land, Ota, Nigeria
***Department of Petroleum Engineering, Covenant University, Canaan land, Ota, Nigeria
****Department of Mechanical Engineering and Science, University of Johannesburg, APK, South Africa

ABSTRACT

This paper introduces a project design on estimating air pollution over geographical regions that have a mono-source of data acquisition. Fifteen years (2000-2013) aerosol optical depth dataset was obtained from the Multi-angle Imaging Spectro-Radiometer (MISR). The peculiar design that has been discussed in this paper focusses on human health and environmental disturbances. The secondary datasets that were generated from the primary data were aerosol loading, particles sizes, Angstrom parameter, and the statistics of the primary dataset. A computational data treatment was introduced for the determination of data reliability of the dataset. The techniques highlighted in this study are germaine to be reproduced in several geographical locations.

INTRODUCTION

Optical properties of aerosols have been found to have a significant influence on the local radiative forcing and radiation balance of the earth (Emetere et al. 2015, Emetere et al. 2016). Basic aerosols optical parameters, such as the extinction and scattering coefficients, the aerosol depth and the single-scattering phase were used to describe aerosol-solar radiation as discussed by Kokhanovsky et al. (2006). The influence of huge aerosols content in the atmosphere are found to be harmful. For example, Dunion and Velden suggested that the Saharan air layer has a significant influence on the intensity and formation of cyclones in the tropical Atlantic region (Dunion & Velden 2004). Goldenberg et al. (2001) examined the causes and implications of aerosols in the formation of Atlantic hurricanes. The information garnered from changes in long-term Saharan dust activities were monitored using information retrieved from dust measurements alongside their concentrations (Prospero & Lamb 2003, Geogdzhayev et al. 2005). Chen et al. (2002) carried out an analysis of fifty years' dataset of global-gauge observation of land precipitations/rainfall in the Sahel region. Like other scientists, it was found that high aerosol loading leads to rainfall anomalies (Emetere 2016 and 2017). Also, Evans et al. (2006) discussed the relationship the outbreak of African dust particulates and Atlantic tropical cyclone activities. These aforementioned works help to buttress the significant effect of aerosols on environmental forces such as hurricanes and activities/performances of cyclones for

filtering or separating/trapping dust particles besides their health implications, influence on agriculture, precipitation (Crippa et al. 2013). For example, in 2012, about 3 million deaths were reported to have been consequential of the inhalation by humans, which was largely responsible for the prominence of cardiovascular and respiratory infections caused by exposures to particulate matter (PM) (Brauer et al. 2012).

Despite much understanding on the atmospheric aerosols, there is a need to understand its long and short-term dangers. Drinovec et al. (2015), with the aid of an Aethalometer carried out accurate measurements of carbon-black aerosols within real time-loading. Vaselovskii et al. (2016), Bovchaliuk et al. (2016) and Rivellini et al. (2017) obtained the optical and physical properties of African dust in Senegal using a multi-wavelength Raman Lidar measurement. In this study, a project design methodology has been suggested for regions of mono-source dataset. For example, there are no or inadequate ground dataset in Bobodioulasso region of Burkina Faso. At the moment, no prior ground studies have been reported in the region. The only source of obtaining aerosol dataset is the use of satellite dataset. The main challenge of adopting mono-source dataset are progressive process error and no validating or control source. In West Africa, it has been shown that the satellite and ground measurement vary significantly over some region (Emetere 2016). Hence, it becomes extremely difficult to rely solely on a mono-source dataset. This paper is to

provide a project design platform for future adoption and a good background study over Bobodioulasso-Burkina Faso. Based on the level of accuracy in the Multi-angle Imaging Spectro-Radiometer (MISR) dataset (Emetere 2017), this paper gives a valid report on the state of air pollution over Bobodioulasso-Burkina Faso.

EXPERIMENTAL DESIGN, MATERIALS AND METHODS

Bobodioulasso is located on latitude 11°10'37.74" N and longitude 4°17'52.44" W (Fig. 1). It is the second largest city in Burkina Faso. The city is known for agricultural trade and textile industry. The research location has a tropical wet and dry climate. The population is fast increasing due to recent development. The primary data were obtained from Multi-angle Imaging Spectro-Radiometer (MISR) as presented in Fig. 2. The raw dataset was initially processed using the Excel program to eliminate missing dataset and calculate the monthly average of the aerosol optical depth (AOD). The processed dataset was subjected to statistical and computational treatment. The computational data treatment was done using the C++ CERN Root codes that were developed to comparatively observe the inter-dependency of the MISR bands. To a large extent, process errors and abnormal data within the dataset can be determined.

The West African regional scale dispersion model (WASDM) for calculating aerosol loading over a region (Emetere et al. 2015):

$$\psi(\lambda) = a_1{}^2 \cos\left(\frac{n_1 \pi \tau(\lambda)}{2} x\right) \cos\left(\frac{n_1 \pi \tau(\lambda)}{2} y\right) +$$
$$\ldots\ldots a_n{}^2 \cos\left(\frac{n_n \pi \tau(\lambda)}{2} x\right) \cos\left(\frac{n_n \pi \tau(\lambda)}{2} y\right) \quad \ldots(1)$$

Where, a is atmospheric constant obtained from the fifteen years aerosol optical depth (AOD) dataset from MISR, n is the tunning constant, $\tau(\lambda)$ is the AOD of the area and $\psi(\lambda)$ is the aerosol loading.

The digital voltage and Angstrom parameters of the study area can be obtained from equation (2) and (3) respectively.

$$I(555) = \frac{I_o(555)}{R^2} \exp(m * \tau(555)) \qquad \ldots(2)$$

Where, I is the solar radiance over the SPM detector at wavelength $\lambda = 555$ nm, I_o is the measure of solar radiation behind the atmosphere, R is the mean Earth-Sun distance in Astronomical Units, τ is the total optical depth (in this case, the average of each month is referred to as the total AOD, and m is the optical air mass.

$$\alpha = -\frac{d \ln(\tau)}{d \ln(\lambda)} \qquad \ldots(3)$$

Where, α is the Angstrom parameter, τ is the aerosol optical depth, and λ is the wavelength.
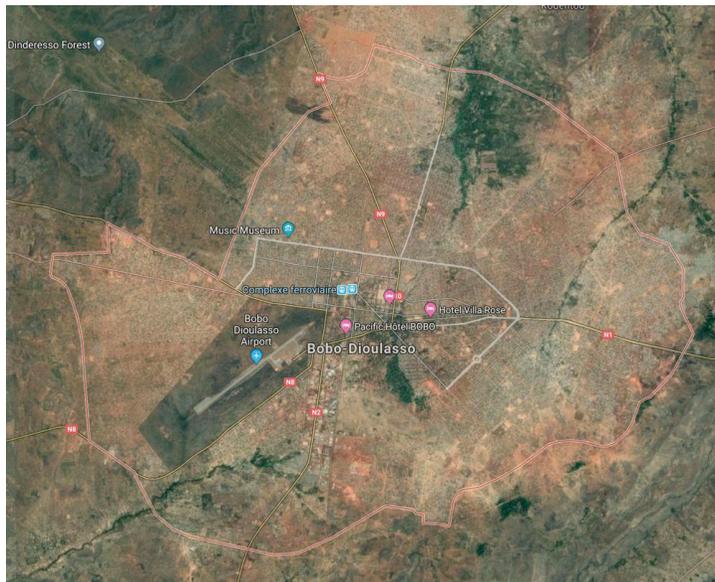
Fig. 1: Google map of Bobodioulasso.

The radius of the particles for atmospheric aerosol and back-envelope was calculated using proposals by Kokhanovsky et al. (2006).

RESULTS AND DISCUSSION

The AOD varied from January down to December as seen in Fig. 2, for all the years. Also in Fig. 2, the AOD was lowest (i.e. approximately 0.18) in November but highest (0.86) in March in the year 2010; no AODs were seen from August to September, in the year 2011, it varied between the value obtained for May (i.e. 0.4) and 0.148 (September), the

highest (0.875) and lowest (0.167) AODs recorded for the year 2012 were those obtained in the months of March and December respectively whereas, no AODs were recorded in the months of July and September. For the year 2013, the highest (0.415) and lowest (0.163) AODs were obtained in the months of March, and January/October respectively with no visible presence of AODs in the months of August and December same year.

The aerosol loading dataset over Bobodioulasso is presented in Fig. 3. From the results shown in Fig. 3, the highest aerosol loading (0.9442) was obtained in the months of January, February, July and August (2000), July and
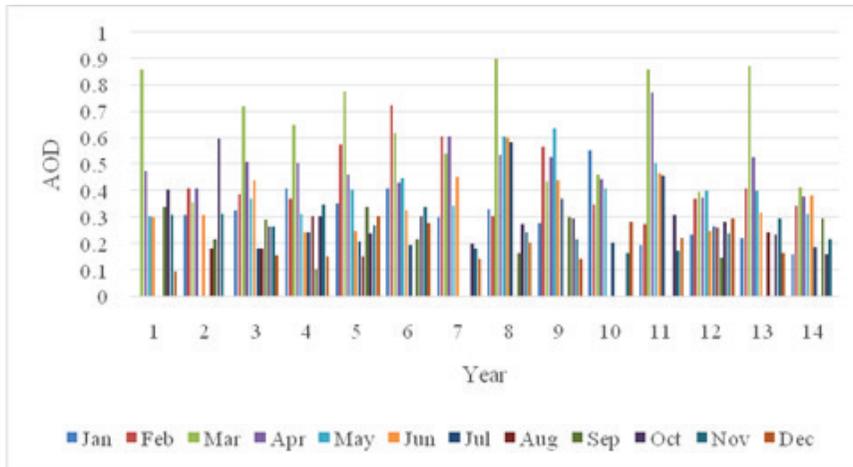
Fig. 2: AOD for Year 2000-2013.
Key: 1-14 = 2000-2013 respectively
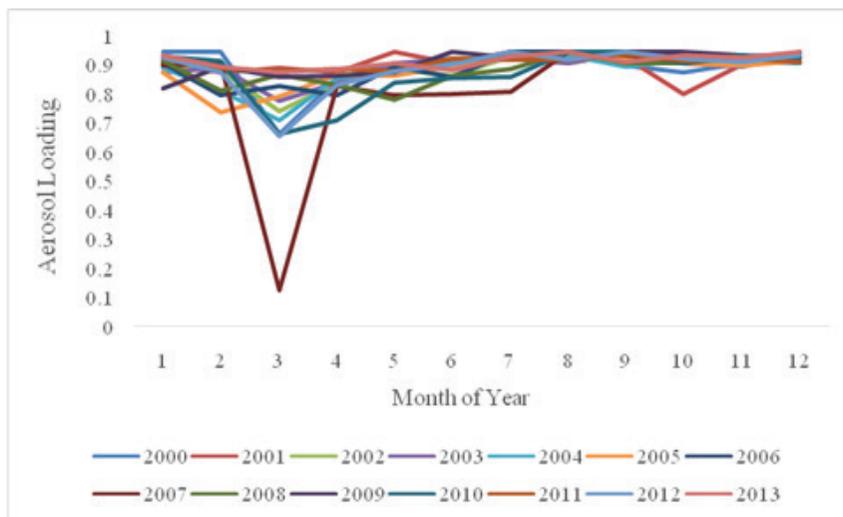
Fig. 3: Aerosol Loading for Year 2000-2013.
Key: 1-12 = Months of the year; from January-December, respectively
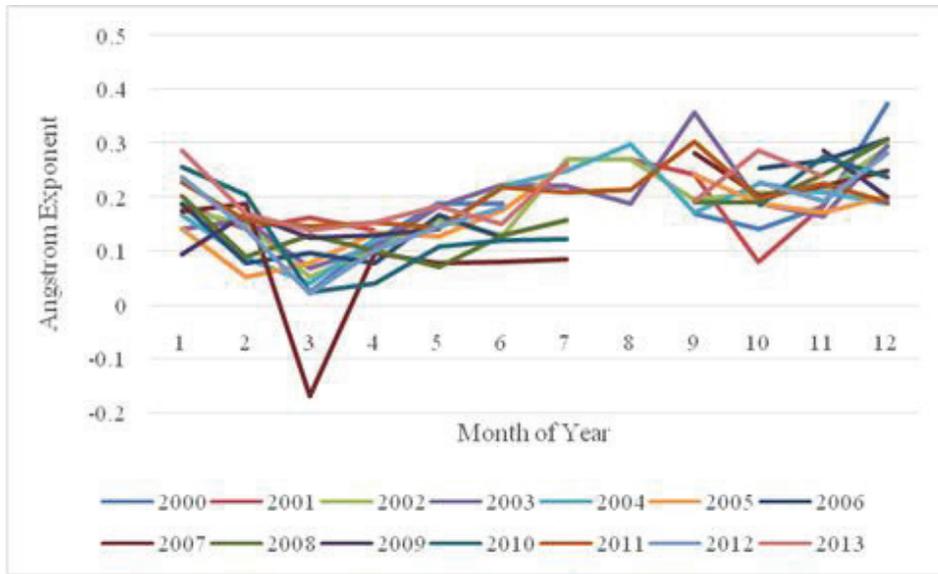
Fig. 4: Angstrom Exponent for Year 2000-2013.
Key: 1-14 = January-December, respectively
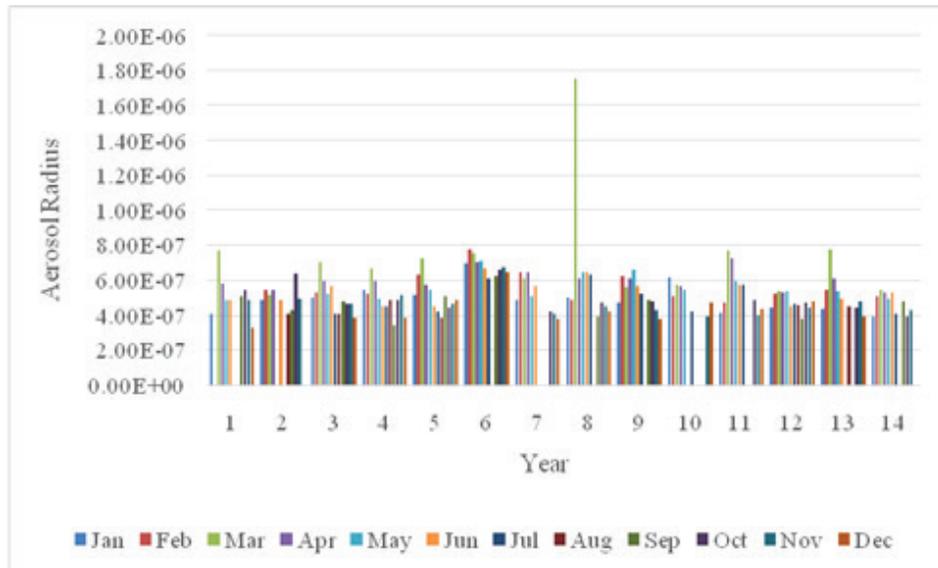
Fig. 5: Aerosol Radius for year 2000-2013.
Key: 1-14 = 2000-2013 respectively

December 2001, August 2005, July-August 2006, August 2007, August 2008 and August-October, 2009 whereas, other values were lower for other months and years.

The Angstrom parameter over Bobodioulasso is presented in Fig. 4. Considering the highest Amstrong value (0.374) recorded in the month of December of the year 2000; it ranges from 0.02 (March)-0.37 (December) in 2000 with no values seen for the months of January, February, July and August of the same year. The values were in the range of 0.08 (October)-0.27 (August) approximately in 2001 with no value recorded for July and December same year, 0.05 (March)-0.293 (December) for 2002, 0.069 (March)-0.296 (December) for 2003 and 0.0399 (March)-0.297 (August) for 2004, 0.05 (February) -0.26

(July) 2005 with no values recorded August of same year, 0.08 (February)-0.31 (December) in 2006, with no values recorded for July-September same year. It ranged between -0.17 (March) and 0.28 (September) in the year 2007 with no Amstrong value recorded for August 2007, from 0.07 (May)-0.31 (December) in 2008 with no value recorded for August 2008. The Amstrong parameter calculated for the year 2009 varies between 0.09 (January) and 0.285 (November) while no values were recorded in the months of June and August-October of same year. It was between 0.02 (March, 2010) and 0.27 (November, 2010) with no visible readings for the month of August-September. It ranged between 0.14 (May, 2011) and 0.3 (September, 2011), it was 0.02 (March)-0.282 (December) for the year 2012 whereas, the values for the months of July and September could not be determined. In 2013, calculated values of the Amstrong parameter are in the range of 0.139 (March) and 0.287 in October 2013 with the values for August and December being indeterminable same year.

The radius of the aerosols that was calculated over the research site is presented in Fig. 6. The statistical treatment of the AOD dataset is presented in Tables 2A-C.

Considering the values in Tables 1A-C, it is evident that, the radius of the particulate aerosols recorded are indicative of particles comprising of fines in the atmospheric region of Bobodioulasso in Senegal.

The mean AOD, confidence interval, variance, standard deviation, coefficient of variation, skew, kurtosis, Kolmogorov Smirnov stat. were estimated. Hence, the instrument is very reliable for taking aerosol property measurements in Bobodioulasso. The estimated AOD properties are dependent on the atmospheric conditions/activities responsible for the distribution of aerosols in the region. Furthermore, the aerosol distribution was skewed to further buttress on the accuracy of the statistical analyses. The years with the least standard deviation and coefficient of variation were indicative of high level of accuracy in the measurements whereas, the years with the highest standard deviation and coefficient of variation were indicative of how inefficiently the instrument could malfunction or give errors in the estimated

Table 1A: AOD statistics over Bobodioulasso from year 2000-2004.

Statistics	2000	2001	2002	2003	2004
Number of values	8	9	12	12	12
Number of missing values	4	3	0	0	0
Minimum	0.094	0.182	0.157	0.105	0.153
Maximum	0.861	0.599	0.722333333	0.6485	0.777333333
Mean	0.386906	0.345564815	0.342708333	0.329937	0.361416667
First quartile	0.30325	0.2865625	0.225333333	0.2455	0.244833333
Third quartile	0.441	0.40925	0.4155	0.38925	0.433333333
Standard error	0.0779726	0.040744465	0.046448295	0.0425115	0.050508824
95% confidence interval	0.184405	0.093956737	0.102232697	0.0935678	0.111169922
99% confidence interval	0.272826	0.136697681	0.144268403	0.132041	0.156880408
Variance	0.0486378	0.014941003	0.025889329	0.0216867	0.030613696
Average deviation	0.14557	0.087720165	0.120048611	0.105969	0.128944444
Standard deviation	0.22054	0.122233396	0.160901613	0.147264	0.174967699
Coefficient of variation	0.57001	0.35372	0.4695	0.44634	0.48412
Skew	1.428	0.897	1.176	0.697	1.345
Kurtosis	3.517	1.612	1.666	0.977	1.852
Kolmogorov-Smirnov stat	0.226	0.182	0.139	0.143	0.189
Critical K-S stat, alpha=.10	0.41	0.387	0.338	0.338	0.338
Critical K-S stat, alpha=.05	0.454	0.43	0.375	0.375	0.375
Critical K-S stat, alpha=.01	0.542	0.513	0.449	0.449	0.449

Table 1B: AOD statistics over Bobodioulasso from year 2005-2009.

Statistics	2005	2006	2007	2008	2009
Number of values	11	9	11	11	8
Number of missing values	1	3	1	1	4
Minimum	0.196	0.1425	0.1675	0.143666667	0.164666667
Maximum	0.724666667	0.609	2.9	0.638	0.555
Mean	0.391121212	0.375888889	0.614681818	0.384242424	0.35959375
First quartile	0.284875	0.195916667	0.253666667	0.28325	0.245375
Third quartile	0.444875	0.556875	0.596125	0.5075	0.4535
Standard error	0.048832139	0.06128345	0.233991981	0.046335619	0.047437703
95% confidence interval	0.108798006	0.141319636	0.521334134	0.103235759	0.112190168
99% confidence interval	0.154749049	0.205605975	0.741520588	0.146837576	0.165984523
Variance	0.026230356	0.033800951	0.602274719	0.023616885	0.018002685
Average deviation	0.12331405	0.157395062	0.415512397	0.126173554	0.10890625
Standard deviation	0.161957884	0.183850351	0.776063605	0.153677862	0.134174086
Coefficient of variation	0.41409	0.48911	1.26255	0.39995	0.37313
Skew	0.981	0.109	3.043	0.164	-0.17
Kurtosis	0.525	-1.772	9.678	-0.859	-1.03
Kolmogorov-Smirnov stat	0.177	0.163	0.414	0.157	0.152
Critical K-S stat, alpha=.10	0.352	0.387	0.352	0.352	0.41
Critical K-S stat, alpha=.05	0.391	0.43	0.391	0.391	0.454
Critical K-S stat, alpha=.01	0.468	0.513	0.468	0.468	0.542

Table 1C: AOD statistics over Bobodioulasso from year 2010-2013.

Statistics	2010	2011	2012	2013
Number of values	10	12	10	10
Number of missing values	2	0	2	2
Minimum	0.176666667	0.148	0.167666667	0.163
Maximum	0.860333333	0.4015	0.87475	0.415
Mean	0.425591667	0.294395833	0.370275	0.286908333
First quartile	0.22475	0.245583333	0.2355	0.188
Third quartile	0.506666667	0.3735	0.411333333	0.38125
Standard error	0.075200385	0.022389481	0.065465378	0.030550013
95% confidence interval	0.170103271	0.049279247	0.148082686	0.06910413
99% confidence interval	0.244401251	0.069541727	0.212762479	0.099287543
Variance	0.056550979	0.006015466	0.042857157	0.009333033
Average deviation	0.188008333	0.062142361	0.146396667	0.08281
Standard deviation	0.237804498	0.077559436	0.207019703	0.096607624
Coefficient of variation	0.55876	0.26345	0.5591	0.33672
Skew	0.879	-0.071	1.816	-0.151
Kurtosis	-0.293	-0.518	3.756	-1.742
Kolmogorov-Smirnov stat	0.185	0.166	0.222	0.158
Critical K-S stat, alpha=.10	0.369	0.338	0.369	0.369
Critical K-S stat, alpha=.05	0.409	0.375	0.409	0.409
Critical K-S stat, alpha=.01	0.489	0.449	0.489	0.489
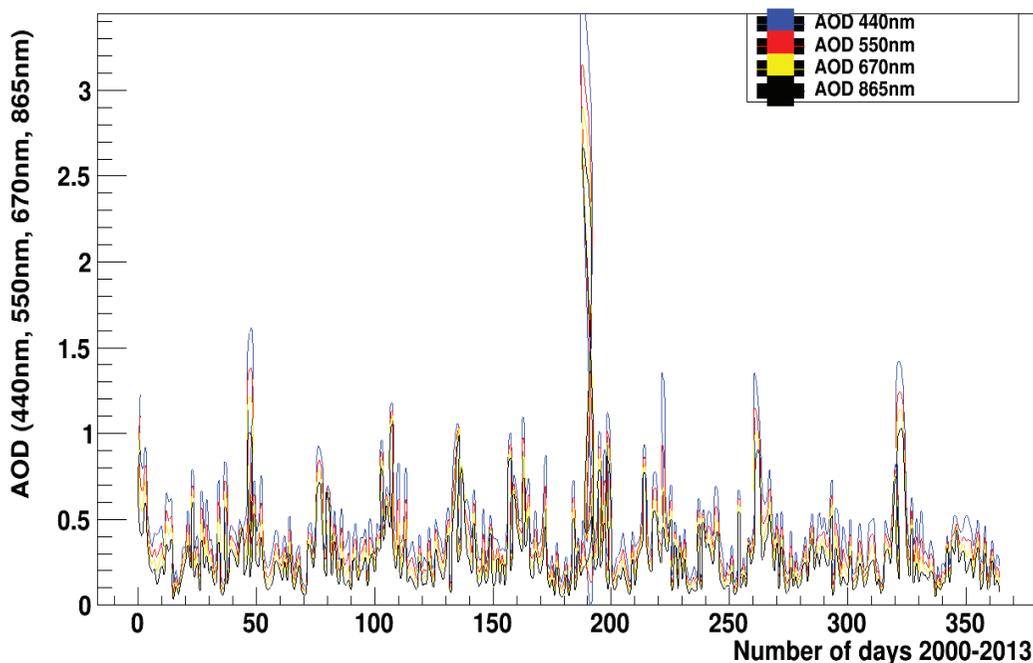
Fig. 6: Comparative analysis of the AOD wavelength of four bands.

values. The recorded average deviations show the influential role the particulate concentration/loading for the years 2000-2013. Also, it can be seen that there is non-uniformity in the coefficient of variation estimated for the years thus, showing an irregularity in the atmospheric distribution of aerosols within the Bobodioulasso region. The years with the highest skews confirmed the tendency for significant effect of aerosols i.e. high tendency for pollution of the surrounding environment of Bobodioulasso.

Standard error of mean is a statement of probability that bothers on how the mean AOD deviates from the average AOD for the years; based on the estimated errors, the accuracy is in the range of 77-98%. Comparing the estimated variances, the estimated AODs for the years show that, the calculated variances are far off the actual mean of the samples by a minimum of 0.06%. The estimated average deviations are a measure of how the AODs deviate from the average AOD in the area. From the estimated standard deviations, one could see the way the measured AODs spread from the mean/median AODs for all the years. The coefficient of variation (i.e. standard deviation/mean), is a measure of the risks involved in trying to get the desired results based on the instrument/equipment used which provides evidence of inaccuracies since the risks are somewhat significant. Skewness is a measure of imbalance or asymmetry of a set of recorded AODs from the mean AODs for the different years, however, it is the degree of distortion

to the left or right of a distribution as well as by how much it differs from a normal distribution. The estimated skews show that the AOD for some years were skewed to the left, hence the AODs recorded do not define a normal distribution but an asymmetric type with more of the recorded AODs positively skewed. Again, since the estimated Kurtosis for the years were more positive than negative which then implies that the AOD distribution was characterized by thick tail compared to a normal distribution hence, it is non-platykurtic/leptokurtic. The estimated Kolmogorov values are a means of knowing if the estimated AODs belong to the same category of data i.e. not measured off the distribution, then, all the recorded values show that they are in order and can actually represent the AOD distribution for the region considered.

The computational data treatments are presented in Figs. 6-9. The computational treatment was a comparative study of the four bands of the AOD dataset obtained from MISR. Fig. 7 shows the 2D plot of the AOD of the four bands. The peak of the graph represents June-July for each of the years. It can be inferred that there are no off-data. Off-data are abnormal data noticed within the dataset. It could be inferred clearly that the highest AOD was found in 2008.

The 3D plots of each band are presented in Fig. 7. It can be observed that the AOD wavelength of 670 & 550 nm and 440 & 550 nm had the highest linearity. However, all plots show that there are relatively low deviations within each
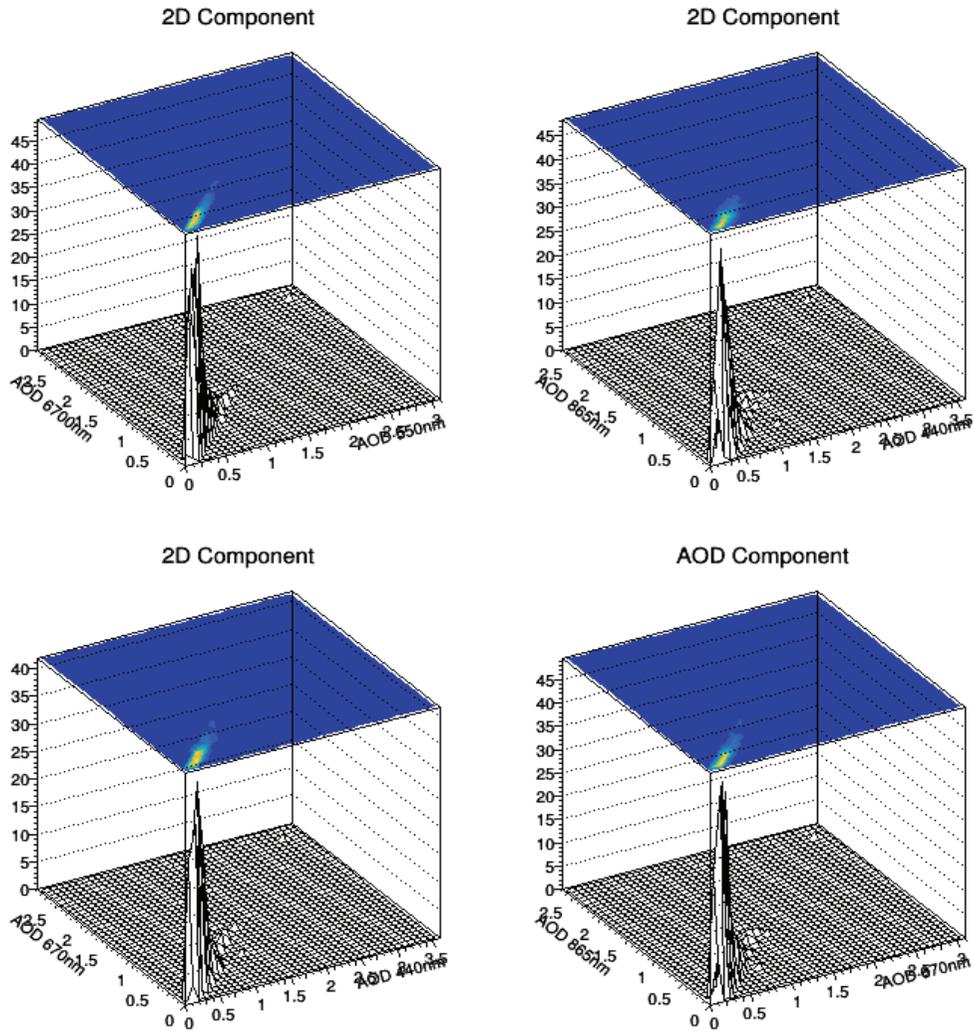
Fig. 7: Interdependency of dataset- 3D outlook.

band. From the statistical treatment, the low deviation can be seen. This means that the dataset is reliable.

The individual dataset distribution was carried-out using the scattered plots presented in Fig. 7. The distribution of all the bands was almost the same. However, the AOD 550 nm, showed a consistent data-spread. Hence, it is computationally logical to conclude that the 550 nm dataset is the most reliable. Lastly, the individual relation of the AOD of each band to the sum of the AOD values of the remaining bands was tested in Figures 8. This type of computational treatment is christened 'linearity test'.

It was further confirmed that AOD 550 nm had the highest linearity. There was no significant deviation from the

linear line from the origin. It was observed that the off-data (separate dot to the right of plot) was present in all the bands. However, it is not significant to alter the results obtained from the dataset.

CONCLUSION

In conclusion, the AOD distribution for the Bobodioulasso region is well represented within a good limit of accuracy. The distribution of aerosols in the region are a measure of the exposure levels and are indicative of potential threats or how insignificant the aerosols in a particular year may be. It was found that the statistical and computational data treatment results showed high correlation. Hence, the reliabili-
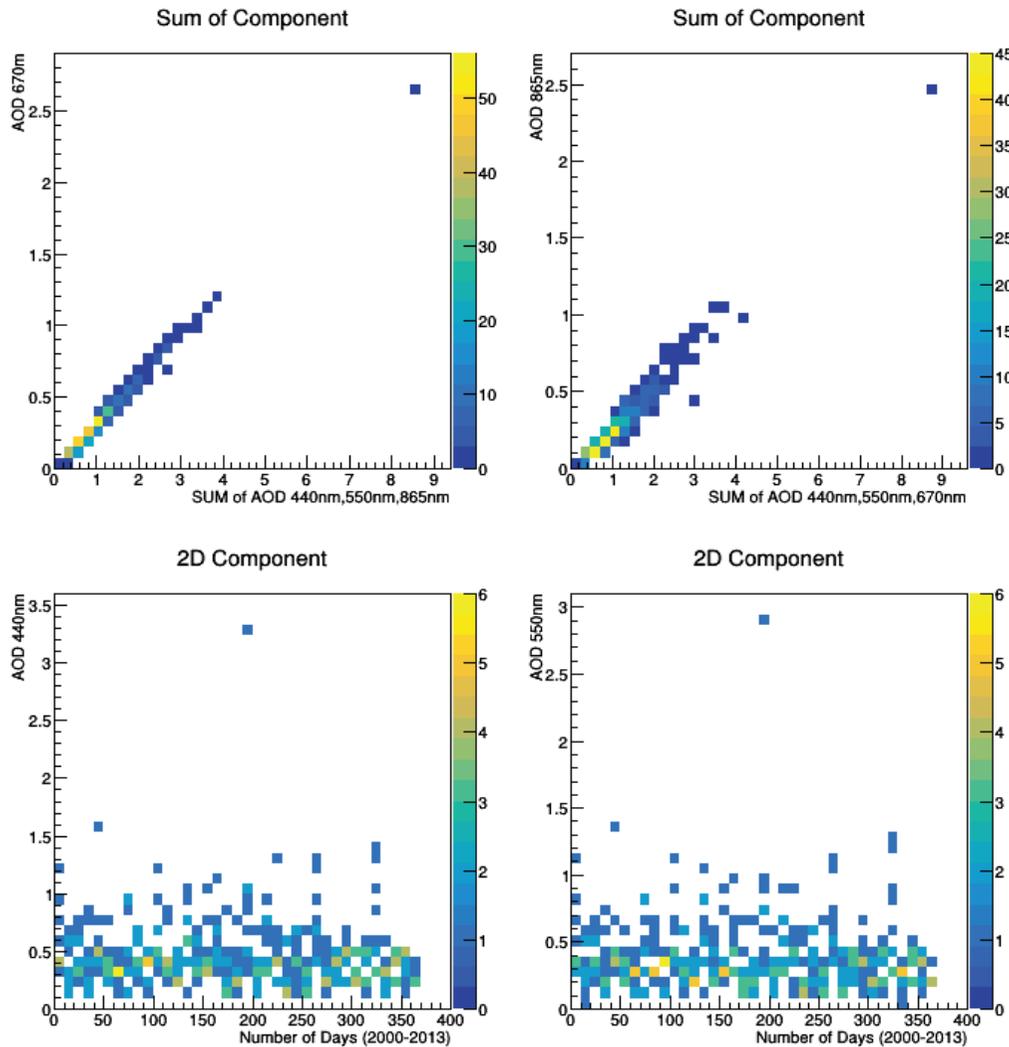
Fig. 8: Interdependency of dataset- scattered plot and linearity test.

ty of a mono-source can be determined. The extensive use of the AOD dataset to determine the aerosol loading angstrom parameter, radius of particulates and back-envelope of aerosol size are indication of how many variables about a geographical region can be determined from mono-source datasets. This paper does not recommend the use of mono-source datasets over a multi-source dataset, it presents a design for carrying-out preliminary studies to guide the main studies over a geographical location.

ACKNOWLEDGEMENT

REFERENCES

Bovchaliuk, V., Goloub, P., Podvin, T., Veselovskii, I., Tanre, D., Chaikovsky, A., Dubovik, O., Mortier, A., Lopatin, A., Korenskiy, M. and Victori, S. 2016. Comparison of aerosol properties retrieved using GARRLiC, LIRIC, and Raman algorithms applied to multi-wavelength lidar and sun/sky-photometer data. Atmospheric Measurements and Technology, 9: 3391-3405

Brauer, M., Amann, M., Burnett, R.T., Cohen, A., Dentener, F., Ezzati, M., Henderson, S.B., Krzyzanowski, M., Martin, R.V., Van-Dingenen, R., Van-Donkelaar, A. and Thurston, G.D. 2012. Exposure assessment for estimation of the global burden of disease attributable to outdoor air pollution. Environmental Science and Technology, 46: 652-660.

Chen, M., Xie, P. and Janowiak, J. 2002. Global land precipitation: A 50-yr monthly analysis based on Gauge observations. Journal of Hydrometeorology, 3: 249-266.

Crippa, M., El Haddad, I., Slowik, J.G., DeCarlo, P.F., Mohr, C., Heringa, M.F., Chirico, R., Marchand, N., Sciare, J. and Baltensperger, U.

2013. Identification of marine and continental aerosol sources in Paris using high resolution aerosol mass spectrometry. Journal of Geophysics Research, 118: 1950-1963.

Drinovec, L., Mocnik, G., Zotter, P., Prévôt, A.S.H., Ruckstuhl, C., Coz, E., Rupakheti, M., Sciare, J., Müller, T., Wiedensohler, A. and Hansen, A.D.A. 2015. The dual-spot Aethalometer: An improved measurement of aerosol black carbon with real-time loading compensation. Atmospheric Measurements and Technology, 8: 1965-1979.

Dunion, J.P. and Velden, C.S. 2004. The impact of the Saharan air layer on Atlantic tropical cyclone activity. Bulletin of American Meteorological Society, 85: 353-365.

Emetere, M.E. 2016. Numerical modelling of west Africa regional scale aerosol dispersion. A doctoral thesis submitted to Covenant University, Nigeria, pp. 65-289.

Emetere, M.E. 2017. Impacts of recirculation event on aerosol dispersion and rainfall patterns in parts of Nigeria. Global Nest Journal, 19(2): 344-352.

Emetere, M.E., Akinyemi, M.L. and Akinojo, O. 2015. Parametric retrieval model for estimating aerosol size distribution via the AERONET, LAGOS station. Environmental Pollution, 207(C): 381-390.

Emetere, M.E., Akinyemi, M.L. and Oladimeji, T.E. 2016. Statistical examination of the aerosols loading over Kano, Nigeria: The satellite observation analysis. Scientific Review Engineering and Environmental Sciences, 72: 167-176.

Evan, A.T., Dunion, J., Foley, J.A., Heidinger, A.K. and Velden, C.S. 2006. New evidence for a relationship between Atlantic tropical cyclone activity and African dust outbreaks. Geophysics Research Letters, 33: L19813

Geogdzhayev, I.V., Mishchenko, M.I., Terez, E.I., Terez, G.A. and Gushchin, G.K. 2005. Regional advanced very high resolution radiometer derived climatology of aerosol optical thickness and size. Journal of Geophysics Research, 110: D23205

Goldenberg, S.B., Landsea, C.W., Mestas-Nunez, W.M. and Gray, W.M. 2001. The recent increase in Atlantic hurricane activity: Causes and implications. Science, 293: 474- 478.

Kokhanovsky, A.A., Hoyningen-Huene, W.V. and Burrows, J.P. 2006. Atmospheric aerosol load as derived from space. Atmospheric Research, 81: 176-185.

Prospero, J.M. and Lamb, P.J. 2003. African droughts and dust transport to the Caribbean: climate change implications. Science, 302: 1024-1027.

Rivellini, L.H., Chiapello, I., Tison, E., Fourmentin, M., Féron, A., Diallo, A., N'Diaye, T., Goloub, P., Canonaco, F., Prévôt, A.S.H. and Riffault, V. 2017. Chemical characterization and source apportionment of submicron aerosols measured in Senegal during the 2015 SHADOW campaign. Atmospheric Chemistry and Physics, 17: 10291-10314.

Veselovskii, I., Goloub, P., Podvin, T., Bovchaliuk, V., Derimian, Y., Augustin, P., Fourmentin, M., Tanre, D., Korenskiy, M., Whiteman, D.N., Diallo, A., Ndiaye, T., Kolgotin, A. and Dubovik, O. 2016. Retrieval of optical and physical properties of African dust from multiwavelength Raman lidar measurements during the SHADOW campaign in Senegal. Atmospheric Chemistry and Physics, 16: 7013-7028